and C(10) determine the conformation of the carbonyl group. If the piperidone ring took up the boat conformation, C(10) would collide with H(11,3) while H(9, 1) and H(8,1) would be forced against H(3) and H(1) respectively, resulting in large compression strains. In all the related compounds whose crystal structures have been determined (Fodor, 1970) the piperidine ring also has the chair conformation.

The mode of packing implies that there is no strong intermolecular hydrogen bonding. The shortest intermolecular contacts range from 2·45 to 2·90 Å between the Cl^- and O atoms of one molecule and the H atoms on surrounding molecules. The O atom is involved in four contacts: 2·47, 2·57, 2·69 and 2·85 Å; Cl^- has two 2·67 and 2·69 Å. None is particularly short and, while these interactions are involved in holding the structure together, they are not hydrogen bonds in the accepted sense (Donohue, 1968).

The unique torsion angles between the H atoms on C atoms 2, 3, 4, 7 and 9 can be used to estimate the coupling constants that will be observed in the n.m.r. spectrum (Jackman & Sternhell, 1969). These values are given in Table 4. A value of 4·5 c.p.s. was observed for $J_{H(3)\cdots H(4)}$ in the free ketone. It thus seems reasonable to conclude that in solution the free ketone retains the conformation found in the solid state for the hydrochloride.

Table 4. *Torsion angles between hydrogen atoms* (±5°)

H(3) ~ H(2,1)	56°	H(4) ~ H(9,1)	74°
H(3) ~ H(2,2)	67	H(3) ~ H(7,1)	36
H(3) ~ H(4)	53	H(3) ~ H(7,2)	85
H(4) ~ H(9,2)	45		

It is a pleasure to acknowledge the interest shown by Dr L. A. Paquette in this project.

This work was supported by grants from the South African Council for Scientific and Industrial Research.

References

Alder, K., Wirtz, H. & Koppelberg, H. (1956). *Ann. Chem.* **601**, 138–154.

Donohue, J. (1968). In *Structural Chemistry and Molecular Biology*, pp. 459–463. San Francisco: Freeman.

Fodor, G. (1970). In *Chemistry of the Alkaloids*, Chap 15, edited by S. W. Pelletier. New York: van Nostrand-Reinhold.

Hughes, E. W. (1941). *J. Amer. Chem. Soc.* **63**, 1737–1752.

International Tables for X-ray Crystallography (1962). Vol. III, pp. 202, 204. Birmingham: Kynoch Press.

Jackman, L. M. & Sternhell, S. (1969). In *Applications of Nuclear Magnetic Resonance Spectroscopy in Organic Chemistry*, 2nd ed. Fig. 4-2-1. Oxford: Pergamon Press.

Laing, M. (1972). *Acta Cryst.* **B28**, 986.

Paquette, L. A. & Heimaster, J. W. (1966). *J. Amer. Chem. Soc.* **88**, 763–768.

Sasaki, T., Eguchi, S. & Kiriyama, T. (1971). *J. Org. Chem.* **36**, 2061–2065.

Schöpf, C. (1937). *Angew. Chem.* **50**, 779–787, 797–805.

Sutton, L. E. (1965). *Tables of Interatomic Distances and Configuration in Molecules and Ions*. London: The Chemical Society.

Acta Cryst. (1975). B31, 2851

The Structure of Halloysite

By G. B. Mitra and S. Bhattacherjee

Department of Physics, Indian Institute of Technology, Kharagpur, India

(*Received* 13 *February* 1975; *accepted* 1 *May* 1975)

A pure sample of Utah halloysite has been subjected to an X-ray diffraction study. The X-ray line profiles have been studied in the light of a theory of diffraction by curved crystals developed in this paper. It is concluded that metahalloysite has a lath-like cylindrical structure and the kaolin layers are considered to be arranged parallel to one another but shifted parallel to themselves. Experimental results have been compared with the theorctical calculations and a satisfactory model with the values of the lattice parameters has been proposed. Observed and calculated line profiles agree with this model fairly satisfactorily.

Introduction

Halloysite is an important member of the kaolin group of clay minerals and is made up of kaolin layers. Brindley & Robinson (1946) have considered it to be composed of kaolin layers which are stacked more or less regularly along the *c* axis but are displaced at random parallel to the *ab* plane. It has not yet been possible to carry out a detailed structural analysis of halloysite because of the great complexity of the diffraction pattern. However, Brindley & Robinson (1948) have made an attempt to analyse the structure of metahalloysite on the basis of a disordered structure. They observed that the X-ray reflexions could be grouped into two categories: (i) the basal reflexions $00l$ which are the only three-dimensional reflexions and

(ii) the two-dimensional *hk* bands. The lattice dimensions were observed to be $b=8{\cdot}90$ and $a=b/\sqrt{3}=5{\cdot}14$ Å. Dimensions of *a* and *b* are practically the same as those of kaolinite but the layer spacing *c* is 7·20 Å which is slightly greater than that for kaolinite.

The same authors also investigated in detail the intensity distribution in the *hk* bands by applying Warren's (1941) theory of diffraction by two-dimensional layer lattices. They observed only a qualitative agreement between the experimental and the theoretical patterns. These differences between the observed and the calculated profiles may be attributed partly to the approximations involved in Warren's (1941) theory and mostly to the inadequacy of the model assumed.

Electron microscopic studies of halloysite first made by Bates, Hildebrand & Swinford (1950) and Bates (1958) have brought to light a new idea regarding the structure of halloysite. These authors have observed that halloysite exhibits tubular morphology rather than the platy one originally suggested. Since then many workers have made thorough electron microscopic studies of halloysite collected from various sources (Bates & Comer, 1955; Brindley, Santos & Santos, 1963; Santos, Santos & Brindley, 1966; *etc.*) and have confirmed the tubular morphology of halloysite.

Bates *et al.* (1950) have attempted to explain the tubular structure in terms of the misfit between the tetrahedral and octahedral sheets of the layer structure. Brindley (1961) has tried to explain the X-ray diffraction from halloysite on the basis of the tubular structure. The high degree of randomness with respect to *a* and *b* axes has been considered in terms of displacements both parallel to the tube axis and around the circumference. The breadth of the basal reflexions has been attributed partly to the small number of layers forming the tube walls and partly to their curvature. Cowley (1961) has also attempted to explain the asymmetric line profiles of metahalloysite on the basis of his theory of curved crystals assuming halloysite to consist of a single curved layer of kaolin and has achieved a partial success.

Thus it appears that while it is extremely likely that the atomic layers in halloysite are curved, no worker has yet been able to propose a convincing model for its structure supported by a suitable theory of diffraction which can satisfactorily explain the experimentally observed X-ray diffraction pattern. In view of this, it was felt that a fresh detailed analysis of the diffraction pattern of halloysite on the basis of a rigorous theory of diffraction by a cluster of curved crystallites might lead to some valuable information on the structure. The present work was therefore undertaken to propose a satisfactory model for the structure of halloysite.

Experimental

A sample of pure halloysite from Utah was selected. The average chemical composition and the result of differential thermal analysis of the sample have already been reported by Bhattacherjee (1971).

The photographic and counter techniques used in the present investigation were similar to those used by Mitra & Bhattacherjee (1969). The powder photographs were used for identification and measurement of interplanar distance while the counter technique was employed for measurement of intensity and study of the line profiles. The background was determined by the method of Mitra & Misra (1966). The order of accuracy achieved for the interplanar distance measurement was about 0·2% while that for the intensity measurement was about 1%. The *d* value corresponding to the first nearly symmetrical peak for the untreated sample was found to be 7·42 Å.

Results and discussions

(*a*) *Nature of the line profiles*

The observed diffraction pattern was found to consist, as reported by Brindley & Robinson (1948), of two different types of profiles: (i) nearly symmetrical peaks usually encountered in diffraction patterns of distorted crystals, (ii) extremely asymmetric broad bands with high background rising sharply in the low-angle side while tapering gradually in the high-angle direction.

All the observed line profiles were corrected for geometrical effect by Stokes's (1948) deconvolution method. Geometrical line profiles for this purpose were constructed by applying the method due to Mitra (1963).

(*b*) *Discussion of the model*

It is well known that halloysite can be considered to have tubular arrangement of atoms. Recently Mitra & Bhattacherjee (1968, 1971) have derived a general expression for the intensity of X-rays diffracted by a powder of fragments of cylindrical crystallites without any simplifying assumptions. The cylindrical crystallites assumed by Mitra (1965) and Mitra & Bhattacherjee (1968, 1971) consist of atoms arranged equiangularly on arcs of concentric circles forming a layer which is repeated at regular intervals. This model, hereinafter called model 1, presupposes that interatomic distances on successive arcs are regularly changing. Such a regular variation in distances between corresponding atoms in successive kaolin layers is difficult to accommodate indefinitely and it will be more realistic to assume the actual distances between corresponding atoms on successive arcs to be the same. This model, hereinafter called model 2, is shown along with model 1 in Fig. 1 (*a*), (*b*).

The essential difference between models 1 and 2 is that while the interatomic arcual distance in different concentric layers in model 2 is constant, that in model 1 varies so that the angle subtended at the centre of the arc is kept constant. Mitra & Bhattacherjee (1974) have considered various ways of achieving model 2 and have concluded that the different constraints in model 2 can be satisfied only if we consider either a small region of the curved part of the crystal or if we assume a series of layer shifts and lattice defects to take place. As a first approximation we may assume the mathematical description in § (*c*) to be valid for model 2. It is well known that the usual straight crystals containing lattice defects can, in the kinematical first approximation, be taken to be one without defects for broad features of the diffraction pattern. Similarly, in the case of curved lattices, we may consider the mathematical description in §(*c*) for model 2 to be valid while in actual practice the treatment will have to be modified as discussed in §§(*f*) and (*h*). Optical transform studies of Mitra & Bhattacherjee (1974) have shown that for all broad features the mathematical description in §(*c*) for model 2 is valid for curved crystals containing various types of lattice defects and hence we proceed to calculate the diffraction intensities on the basis of the mathematical description of model 2 given in §(*c*).

(*c*) *Diffraction intensities from cluster of curved crystallites of model* 2

Let the crystallite consist, as in Fig. 1(*b*), of layers *ABCD* separated by *c* in the *Z* direction. Then the position of the *n*th atom in the *m*th arc on the *t*th layer $\boldsymbol{\varrho}_{mnt}$ will be described by the cylindrical coordinates $(R+mb)$, $n\varphi_m$ and tc respectively, where R is the radius of the first arc from the common centre on the *t*th layer; b has been taken to be equal to the distance between successive arcs which is justified on the assumption that the crystallite is of small size and of small curvature as discussed in the previous section and in Mitra & Bhattacherjee (1974). φ_m and φ_0 are the angular distances between two nearest neighbour points on the *m*th and the first arcs respectively. In terms of the cartesian reference system (*XYZ*) shown in Fig. 2(*a*), (*b*).

$$\boldsymbol{\varrho}_{mnt}=\mathbf{i}_x(R+mb)\sin n\varphi_m+\mathbf{i}_y(R+mb)\cos n\varphi_m+\mathbf{i}_z tc \quad (1)$$

where $\mathbf{i}_x$, $\mathbf{i}_y$ and $\mathbf{i}_z$ are unit vectors in the directions X, Y and Z respectively. Let the unit vectors in the directions of the incident and diffracted beams be $\boldsymbol{\sigma}_0$ and $\boldsymbol{\sigma}_d$ respectively, let us define $\boldsymbol{\sigma}$ as $\boldsymbol{\sigma}=\boldsymbol{\sigma}_d-\boldsymbol{\sigma}_0$ and let $\boldsymbol{\sigma}$ be described by the spherical coordinates S, χ and γ respectively, so that in terms of the Cartesian axes

$$\boldsymbol{\sigma}=\mathbf{i}_x S\sin\gamma\cos\chi+\mathbf{i}_y S\sin\gamma\sin\chi+\mathbf{i}_z S\cos\gamma\,. \quad (2)$$

Then the amplitude of the X-rays diffracted in the direction $\boldsymbol{\sigma}$ will be given by

$$A(\boldsymbol{\sigma})=F(\boldsymbol{\sigma})\sum_{m=0}^{M-1}\sum_{n=0}^{N-1}\sum_{t=0}^{T-1}\exp\left\{i\frac{2\pi}{\lambda}(\boldsymbol{\varrho}_{mnt}-\boldsymbol{\varrho}_0)\cdot\boldsymbol{\sigma}\right\} \quad (3)$$

where $F(\boldsymbol{\sigma})$ is the amplitude of the X-rays scattered by the identical group of atoms attached to each lattice point (say P) and $\boldsymbol{\varrho}_0$ locates the position of the atom at the origin $(R,0,0)$. It is easily seen that

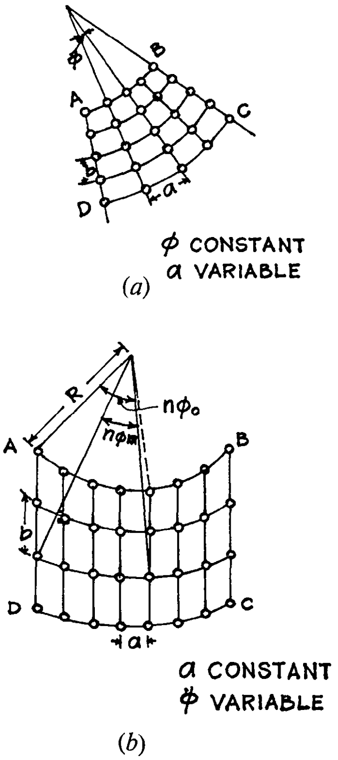

(*a*)

(*b*)

Fig. 1. Models of curved lattice. (*a*) Model 1. (*b*) Model 2.

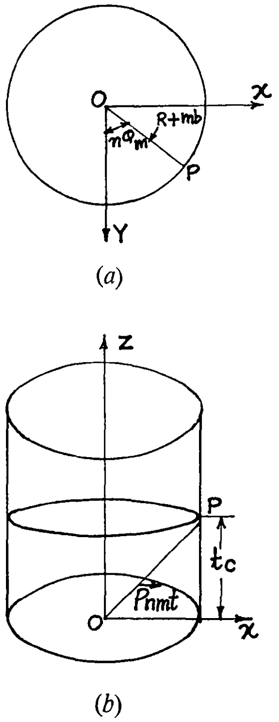

(*a*)

(*b*)

Fig. 2. (*a*) Position of the lattice site in *XY* plane. (*b*) Cylindrical shell with axis parallel to *OZ*. $\boldsymbol{\varrho}_{mnt}$ denotes the position of the lattice site *P* from the origin *O* in the coordinate system *XYZ*.

$$A(\boldsymbol{\sigma})=F(\boldsymbol{\sigma})G(\boldsymbol{\sigma})\frac{\sin\left(\frac{\pi}{\lambda}T\mathbf{c}\,.\,\boldsymbol{\sigma}\right)}{\sin\left(\frac{\pi}{\lambda}\mathbf{c}\,.\,\boldsymbol{\sigma}\right)}$$

$$\times\exp\left\{-\frac{2\pi}{\lambda}i\left(\mathbf{R}-\left(\frac{T-1}{2}\right)\mathbf{c}\right).\,\boldsymbol{\sigma}\right\} \qquad (4)$$

where

$$G(\boldsymbol{\sigma})=\sum_{m=0}^{M-1}\sum_{n=0}^{N-1}\exp\left(i\frac{2\pi}{\lambda}\boldsymbol{\varrho}_{mn}\,.\,\boldsymbol{\sigma}\right) \qquad (5)$$

with

$$\boldsymbol{\varrho}_{mnt}=\boldsymbol{\varrho}_{mn}+t\mathbf{c}\,. \qquad (6)$$

It is clear from equations (1), (2) and (5) that

$$G(\mathbf{s})=\sum_{n=0}^{N-1}\sum_{m=0}^{M-1}\exp\left\{i\frac{2\pi}{\lambda}(R+mb)S\sin\gamma\sin(n\varphi_m+\chi)\right\}. \qquad (7)$$

Proceeding as Mitra (1965) we obtain

$$G(\mu)=\sum_{n=0}^{N-1}\sum_{m=0}^{M-1}\sum_{p=-\infty}^{+\infty}J_p(\mu[R+mb])\exp ip(n\varphi_m+\chi) \quad (8)$$

where $J_p(x)$ is the Bessel function of the first kind of order p and argument x; p is an integer and $M=(2\pi/\lambda)S\sin\gamma=(4\pi/\lambda)\sin\theta\sin\gamma$ since $|\boldsymbol{\sigma}|=S=2\sin\theta$, 2θ being the angle between $\boldsymbol{\sigma}_d$ and $\boldsymbol{\sigma}_0$. The intensity $I(\boldsymbol{\sigma})$ in the direction $\boldsymbol{\sigma}$ is given by

$$I(\boldsymbol{\sigma})=A(\boldsymbol{\sigma})A^*(\boldsymbol{\sigma})$$

$$=F(\boldsymbol{\sigma})F^*(\boldsymbol{\sigma})H(\boldsymbol{\sigma})\frac{\sin^2\left(\frac{\pi}{\lambda}T\mathbf{c}\,.\,\boldsymbol{\sigma}\right)}{\sin^2\left(\frac{\pi}{\lambda}\mathbf{c}\,.\,\boldsymbol{\sigma}\right)} \qquad (9)$$

where

$$H(\boldsymbol{\sigma})=G(\boldsymbol{\sigma})G^*(\boldsymbol{\sigma})\,.$$

It is clear from equation (9) that $I(\boldsymbol{\sigma})$ will have non-zero values for a given value of θ only if

$$\frac{2\pi}{\lambda}c\sin\theta\cos\gamma=l_0 \qquad (10)$$

where l_0 is an integer. Thus for a given value of θ only certain values of γ will be permitted. Hence the average intensity diffracted at a given angle 2θ due to all orientations of the crystallites means averaging over all values of χ and only these permitted values of γ, the average value of $H(\boldsymbol{\sigma})$ for a given value of θ but all values of χ will be given by

$$H(\mu)=\sum_p\sum_n\sum_{n'}\sum_m\sum_{m'}J_p(\mu[R+mb])J_p(\mu[R+m'b])$$

$$\times\exp ip(n\varphi_m-n'\varphi_{m'})=\sum_n\sum_{n'}\sum_m\sum_{m'}J_0(z) \qquad (11)$$

where

$$z^2=\mu^2[(R+mb)^2+(R+m'b)^2-2(R+mb)(R+m'b)$$

$$\times\cos(n\varphi_m-n'\varphi_{m'})]\,. \qquad (12)$$

Since, as shown by Morse & Fesbach (1953),

$$J_0(z)=\sum_{p=-\infty}^{+\infty}J_p(x)J_p(y)\exp(ip\varphi)$$

with

$$z^2=x^2+y^2-2xy\cos\varphi\,.$$

In the corresponding expression for model 1, equations (9), (10) and (11) will remain unchanged while equation (12) will be modified by putting $\varphi_m=\varphi_0$. Now in model 2

$$\varphi_m=\frac{a}{R+mb}\,;\quad\varphi_0=\frac{a}{R}$$

or

$$\varphi_m=\frac{\varphi_0}{1+mr_2\varphi_0}$$

where $r_2=b/a$ and a the constant arcual distance between two nearest neighbour lattice points on the same arc. Thus when $mr_2\varphi_0\ll1$, *i.e.* R very large, the intensity expressions for the two models become identical.

Introducing

$$Q=\frac{2\pi}{N\varphi_0}\,;\quad h'=\frac{2a\sin\theta}{\lambda}$$

and

$$r_1=\frac{c}{a}$$

we have

$$I(h')=F^2(h')\sum_{l_0}\frac{\sin^2(\pi Tl_0)}{\sin^2(\pi l_0)}$$

$$\times\sum_m\sum_{m'}\sum_n\sum_{n'}J_0\left(QNh'\sqrt{\left(1-\frac{l_0^2}{r_1^2h'^2}\right)}\right.$$

$$\times\sqrt{\Big[}(1+mr_2\varphi_0)^2+(1+m'r_2\varphi_0)^2-2(1+mr_2\varphi_0)$$

$$\left.\times(1+m'r_2\varphi_0)\cos\frac{2\pi}{QN}\left\{\frac{n}{1+mr_2\varphi_0}-\frac{n'}{1+m'r_2\varphi_0}\right\}\Big]\right). \qquad (13)$$

The summation over l_0 is carried over all values of l_0 permitted by equation (10).

(*d*) *Nature of intensity distribution from cluster of curved crystallites of model* 2

Results of numerical computations of $I(h'l_0)$ for several cases, *viz.* $N=20$, $N\varphi=10°$, $r_1=1$ and 2, $r_2=1$, $M=1$ and $l_0=0,1,2$, show that the general behaviour of $I(h'l_0)$ with h' for different values of l_0 is nearly the same for both models 1 and 2. Since these results have been shown graphically for model 1 by Mitra & Bhattacherjee (1971) they have not been reproduced here. However, overall values of $I(h')$ for different values of l_0 and large T for some of these cases are shown in Fig. 3. It should be mentioned here that for the present calculation M has been taken to be only 1 in order to facilitate the calculations. This approach has been amply demonstrated in the optical diffraction study by Mitra & Bhattacherjee (1974) and by calculation by Bhattacherjee & Mathur (1974).

From these curves and equation (13) it is clear that the maximum will be obtained at $h' = l_0/r_1$ *i.e.*, $2a \sin \theta/\lambda = l_0 a/c$ or $2c \sin \theta/\lambda = l_0$. This means that the maximum for $l_0 = 0$ will be at $\sin \theta = 0$; for $l_0 = 1$ will be at $\sin \theta = \lambda/2c$ *etc.* $I(h'l_0)$ at these values of h' becomes $T^2N^2M^2F^2(h')$. Thus the location of maxima from such crystallites in experimental curves should immediately lead to the determination of c, which is found to have a value of 4·95 Å [see §(*e*)].

(*e*) *Comparison with experimental intensity distribution from metahalloysite*

As has been mentioned earlier the observed diffraction peaks from metahalloysite consist of (i) some nearly symmetrical peaks and (ii) some highly asymmetric peaks. Peaks of type (ii) can be attributed to the curved crystallites as shown in Fig. 4. Reflexions shown in Fig. 4(*b*) will be of the usual Bragg type but slightly broadened due to stacking faults. The stacking fault clearly consists of shift of a layer with respect to its neighbouring layer. These reflexions will be broad but symmetrical. Peaks of type (i) may be attributed to such reflexions. Clearly, the value of a can be obtained from the position of the symmetrical peaks.

Since these nearly symmetrical peaks correspond to an interlayer distance of 7·4 Å and its various submultiples, it is clear that $a = 7{\cdot}4$ Å. This is further confirmed from the comparison of locations of the different peaks of type (ii) in the observed as well as calculated diffraction patterns as shown in Table 1 and Fig. 5(*a*), (*b*).

Table 1. *Values of 'a' as determined by comparing the locations of the asymmetric peaks in the observed as well as calculated diffraction patterns*

Asymmetric peaks	h'	θ (°)	'a'
First (02, 11)	1·74	10·1	7·6 Å
2nd (20, 13)	3·35	19·2	7·8
3rd (31, 15, 24)	4·25	27·4	7·1
4th (06, 33)	4·92	31·3	7·3

Again, as shown in §(*d*) the location of the first asymmetric peak will reveal the value of c. Since the first asymmetric peak corresponds to $2\theta = 19°$ we have $c = 4{\cdot}95$ Å. Thus a and c of the curved crystallite have the same values as c and a of the traditional kaolin layer; b in the curved crystal may be taken to be the same as in the traditional case.

(*f*) *Discussion on the structure of metahalloysite*

We thus find that metahalloysite consists of kaolin layers shifted in the **b** direction resulting in a curvature in the *ab* plane. Such shifts have been observed for kaolinite (Mitra, 1963) and its dehydration products (Mitra & Bhattacherjee, 1970). Since the bond between the kaolin layers is very weak, there are likely to be such shifts and also tilts and variation in interlayer distances. Brindley (1955) and Cowley (1961) have assumed that the kaolin layers themselves are curved. This means that b of the curved crystal will have the value 7·4 Å. But it has already been found in §(*e*) that the observed diffraction pattern is consistent with $a = 7{\cdot}4$ Å. It is difficult, with the accepted ideas about the kaolin layers, to reconcile both these values and it is extremely likely that the model proposed by Brindley (1955) and Cowley (1961) is wrong as far as metahalloysite is concerned. It may be valid for hydrated halloysite. The curvature of the kaolin layers has been assumed because of the misfit between the silica tetrahedra and alumina octahedra. Such curvature is not inconsistent with the model discussed here and the theory developed in §(*c*) will still be applicable to it provided the curvature is not large. In fact, as has been discussed in §(*b*), this curvature of the kaolin layers [shown in Fig. 6(*b*)] is an essential feature of the model proposed in this paper. We as-

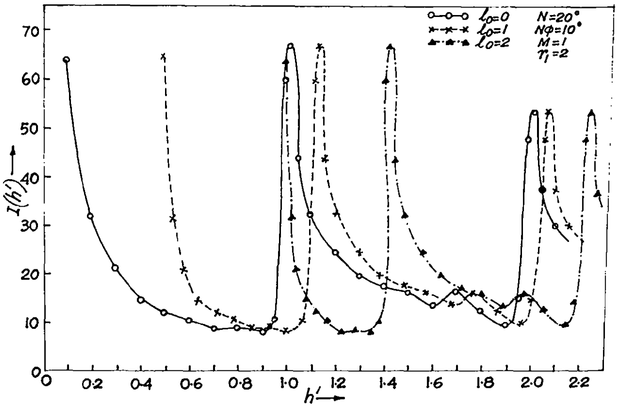

Fig. 3. Plot of $I(h)$ *vs* h for a random aggregate of identical shell fragments with a given angular opening.

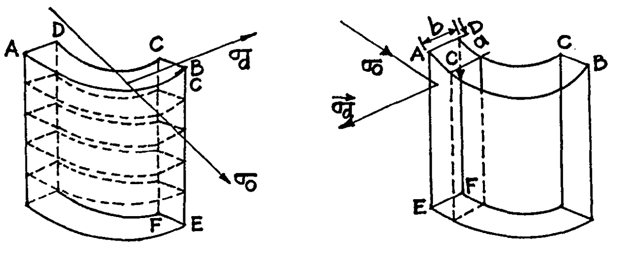

(*a*) (*b*)

Fig. 4. X-ray reflexions from different faces of a curved crystallite. (*a*) Reflexions responsible for asymmetric bands. (*b*) Reflexions responsible for the nearly symmetrical peaks.

sume this curvature to be very small, so that, as shown by Mitra (1965), the usual Laue–Bragg laws are valid for this case. The slight anisotropy of the peaks of type (i) is presumably due to this curvature which may also be taken to give rise to variability in interlayer spacings as has been observed by Bhattacherjee (1973).

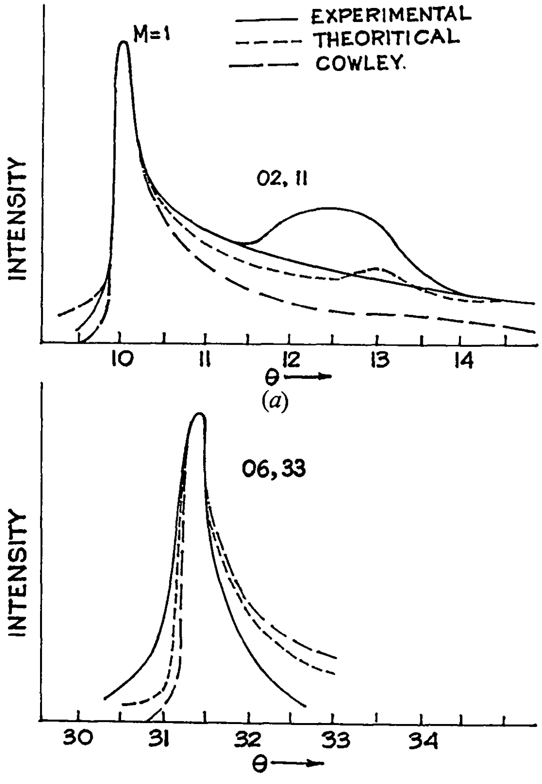

(a)

(b)

Fig. 5. Experimental diffraction profiles of the asymmetric bands along with the theoretical profiles calculated on the basis of equation (13).

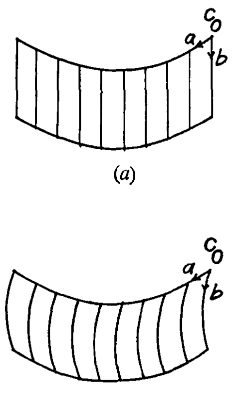

(a)

(b)

Fig. 6. Kaolin layers in metahalloysite according to the model proposed. (*a*) Metahalloysite crystallite having curvature in the *ab* plane caused by the shift of the kaolin layers parallel to **b**. (*b*) Curvature of the kaolin layers.

(*g*) *Curvature as a result of interlayer shift*

A simple relation between the curvature of the metahalloysite crystals and the probability of shift of the kaolin layer in the **b** direction by an amount $\frac{1}{3}b$ can easily be established. Thus if N is the total number of kaolin layers constituting the curved-lath-like halloysite crystallite and P the probability of interlayer shift, the average shift per layer will be $\frac{1}{3}bP$. If R is the radius of curvature then

$$2R\tfrac{1}{3}bP=a^2 \qquad (14)$$

or

$$R=\tfrac{3}{2}\frac{a^2}{bP}$$

and

$$\varphi N=\frac{Na}{R}=\tfrac{2}{3}\frac{NbP}{a}=\tfrac{2}{3}NPr_2\,. \qquad (15)$$

When $P=1$, *i.e.* each layer is shifted with respect to its neighbour, the full cylinder is formed when

$$2\pi=\tfrac{2}{3}Nr_2$$

or

$$N=\frac{3\pi}{r_2} \qquad (16)$$

which is usually a very small number. When the probability of shift is P, the maximum number of layers which can be accommodated in a cylinder is $3\pi/Pr_2$. If N is larger than this and the layer shift proceeds unabated with probability P, the lath is likely to break into a number of cylinders and laths depending on the value of N. The halloysite crystallite is not thus taken to be a smooth cylindrical lath but a serrated cylindrical one.

(*h*) *Diffraction intensities due to serrated cylinders*

The effect on the diffraction pattern of the halloysite cylinder being serrated instead of smooth is that R in equations (1) and (7) is no longer constant for all values of n but will be $R+\Delta R_n$ for the nth layer, ΔR_n being a small value. The terms involving ΔR_n can be absorbed in $F(\sigma)$ so that $F(\sigma)$ is different for different values of n. In equation (9) $F(\sigma)F^*(\sigma)$ will now be replaced by the average value $\langle F_n(\sigma)F^*_{n'}(\sigma)\rangle$; the averaging process being carried over all values of n and n'. This result is exactly the same as that obtained in the case of layer shift in normal straight crystals. As in the analogous case of the straight crystals, the main features of the diffraction pattern will be unaltered by the serrations in the cylindrical crystals – only the line profile will be slightly modified. The resulting modification in the line profile will be discussed in a forthcoming publication. For the present, however, the determination of a, b and c in §(*e*) above will be unaffected by the modification in the model of the cylindrical crystallites.

(*i*) *Comparison between experimental and calculated line profiles*

Fig. 5(*a*), (*b*) shows the experimental profiles of the two asymmetric bands (02, 11 and 06, 33) in the angular regions $\theta = 9\text{–}14°$ and 30–33° along with the theoretical curves based on equation (13) with $N = 20$, $r_1 = 0{\cdot}7$ corresponding to $c = 5{\cdot}14$ Å, $a = 7{\cdot}4$ Å, $N\varphi = 10°$ and $M = 1$ for $h' = 1{\cdot}7\text{–}1{\cdot}9$ and 4·85–5·50. In the model of curved halloysite envisaged in the present work, the value of b which is the same as in kaolinite has been assumed to remain unchanged. Hence our main interest has been to obtain values of a and c of the curved model and for this calculation, as has been shown by Mitra & Bhattacherjee (1974) and Bhattacherjee & Mathur (1974), $M > 1$ does not yield results which are essentially different from those of $M = 1$.

Diffraction profiles in these angular ranges as calculated by Cowley (1961) have also been reproduced in the same figures for the sake of comparison. It is found that the theoretical curves based on equation (13) agree quite well with the experimental curves. It is further evident from Fig. 5(*b*) that the agreement between the theoretical and experimental profiles is much better than that of obtained by Brindley & Robinson (1948) by the application of Warren's theory of disordered lattice. Fig. 5(*b*) also shows that the agreement between the calculated and the observed profiles in the present case is evidently better than that of Cowley (1961). Brindley & Robinson (1948) found that the half intensity width of the theoretical curve on the basis of Warren's theory is half that of the experimental curve of Fig. 5(*b*). In the present case, however, the half width of the theoretical curve is equal to the experimental half width [Fig. 5(*b*)]. In case of Fig. 5(*a*) too, the agreement between the theoretical and the experimental curves is fairly good and this agreement is better than that calculated either from Warren's theory or from Cowley's.

Conclusions

The above discussion enables us to arrive at certain definite conclusions regarding the structure of metahalloysite. It is observed that the theory of diffraction by curved crystallites developed in this paper can explain more satisfactorily the experimental results than Warren's theory of diffraction by a disordered stack of two-dimensional layers. We can now safely conclude that metahalloysite has a cylindrical lattice and is made up of a stacking of annular layers with a spacing of 4·95 Å between consecutive layers. Each annular layer is composed of arcs consisting of about 20 atoms equiangularly placed. The angle made by the first arc on the concave side at the axis of the cylinder is very small (~10°) and the arcual distance between two neighbouring atoms is 7·42 Å. The arcual distance between two neighbouring atoms on each arc remains the same so that the angle subtended at the axis of the cylinder is different for different arcs. The kaolin layers which are arranged parallel to each other are slightly curved and shift sufficiently parallel to themselves so that the cylinder is formed.

We wish to thank Dr George Switzer, Smithsonian Institution, U.S.A., for the gift of the sample (Cat. No. 106236).

References

Bates, T. F. (1958). *Selected Electron Micrographs of Clay and Other Fine-grained Minerals*, Circular No. 51, College of Mineral Industries, Pennsylvania State Univ.

Bates, T. F. & Comer, J. J. (1955). *Electron Microscopy of Clay Surface. Clays and Clay Minerals*, edited by W. O. Milligan, pp. 1–25. Publication 395, Nat. Acad. Sci. Res. Counc. Washington.

Bates, T. F., Hildebrand, F. A. & Swinford, A. (1950). *Amer. Min.* **35**, 463–484.

Bhattacherjee, S. (1971). *Ind. J. Pure Appl. Phys.* **9**, 1054–1056.

Bhattacherjee, S. (1973). *Proc. Natl. Acad. Sci.* **39**A, 54–61.

Bhattacherjee, S. & Mathur, B. K. (1974). *Ind. J. Pure Appl. Phys.* **12**, 230–232.

Brindley, G. W. (1955). *Structural Mineralogy of Clays. Clays and Clay Technology*, edited by J. A. Pask & M. D. Turner, Bulletin 169, pp. 33–43. California Division of Mines, San Francisco.

Brindley, G. W. (1961). *The X-ray Identification and Crystal Structure of Clay Minerals*, edited by G. Brown, pp. 72–73. London: The Mineralogical Society.

Brindley, G. W. & Robinson, K. (1946). *Trans. Faraday Soc.* **42**B, 198–205.

Brindley, G. W. & Robinson, K. (1948). *Miner. Mag.* **28**, 393–407.

Brindley, G. W., Santos, P. de Souza & Santos, H. de Souza (1963). *Amer. Min.* **48**, 897–910.

Cowley, J. H. (1961). *Acta Cryst.* **14**, 920–927.

Mitra, G. B. (1963). *Z. Kristallogr.* **119**, 161–175.

Mitra, G. B. (1965). *Acta Cryst.* **18**, 464–467.

Mitra, G. B. & Bhattacherjee, S. (1968). *Acta Cryst.* A**24**, 266–269.

Mitra, G. B. & Bhattacherjee, S. (1969). *Amer. Min.* **54**, 1409.

Mitra, G. B. & Bhattacherjee, S. (1970). *Acta Cryst.* B**26**, 2124–2128.

Mitra, G. B. & Bhattacherjee, S. (1971). *Acta Cryst.* A**27**, 22–28.

Mitra, G. B. & Bhattacherjee, S. (1974). *Ind. J. Phys.* **48**, 520–528.

Mitra, G. B. & Misra, N. K. (1966). *Brit. J. Appl. Phys.* **17**, 1319–1328.

Morse, M. P. & Feshbach, H. (1953). *Methods of Theoretical Physics*, p. 621. Tokyo: McGraw-Hill.

Santos, P. de Souza, Santos, H. de Souza & Brindley, G. W. (1960). *Amer. Min.* **51**, 1640–1648.

Stokes, A. R. (1948). *Proc. Phys. Soc.* **61**, 382–391.

Warren, B. E. (1941). *Phys. Rev.* **59**, 693–698.